Electronic Supplementary Material (ESI) for Journal of Materials Chemistry C.

Supporting Information

Fabricating Ultra-Flexible Photodetectors at Neutral Mechanical Plane by Encapsulation

Guomin Ding,[a] Honglei Chen,[b] Zuxi Yu,[b] Nan Liu,[c] and Min Wang*[a]

[a] College of Materials Science and Technology, Nanjing University of Aeronautics and Astronautics, Nanjing 210016, People's Republic of China
[b] School of Materials Science and Engineering, Hefei University of Technology, Tunxi Road 193, Hefei, 230009, People's Republic of China
[c] College of Chemistry, Beijing Normal University, Beijing, 100875, People's Republic of China
* Correspondence author: Min Wang. E-mail address: minwang@nuaa.edu.cn.

1. Morphology characterization of CdS films on PET substrate by AFM

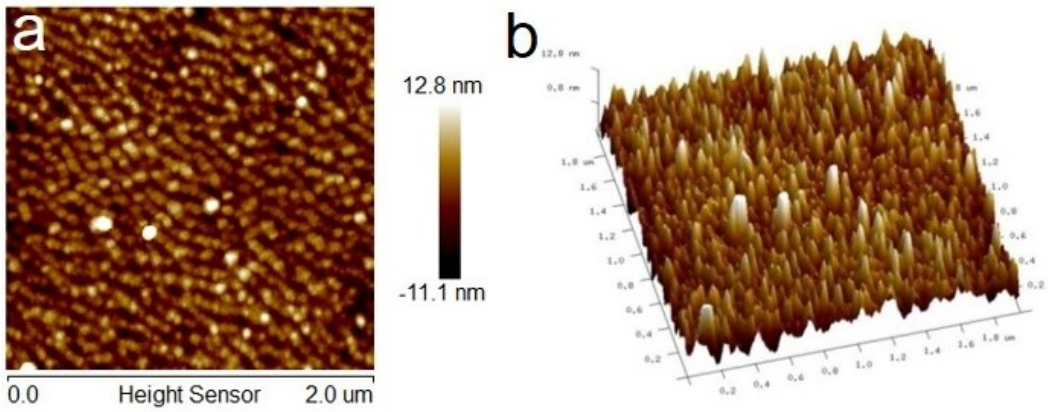

Fig. S1. (a) 2D and (b) 3D AFM images of CdS films deposited on PET substrate. The results show that the as-deposited CdS films consist of CdS nanoparticles with diameter of ~30 nm.

2. XRD patterns of CdS films on PET substrate

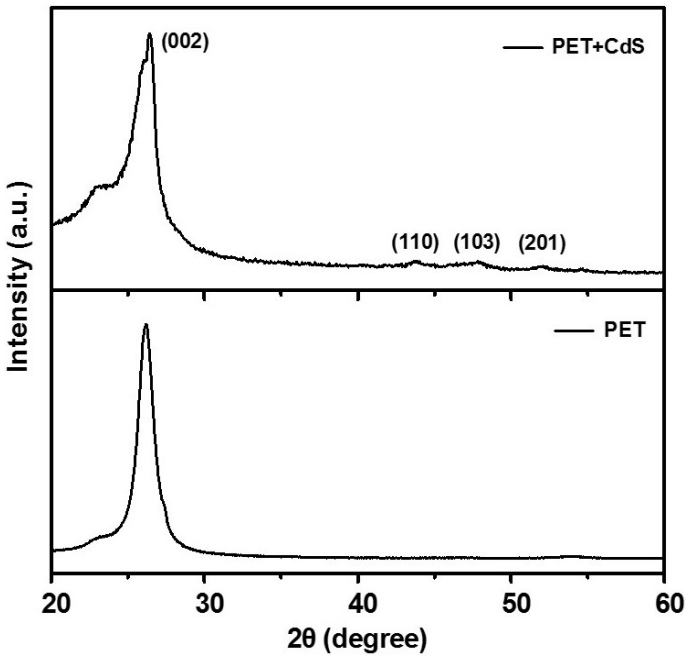

Fig. S2. The peaks around 26.4, 43.7, 47.9 and 52.0 degree correspond to (002), (110), (103) and (201) of CdS, showing that the deposition of CdS films with pure phase have been succeeded.

3. XPS characterization of CdS films deposited on PET substrate

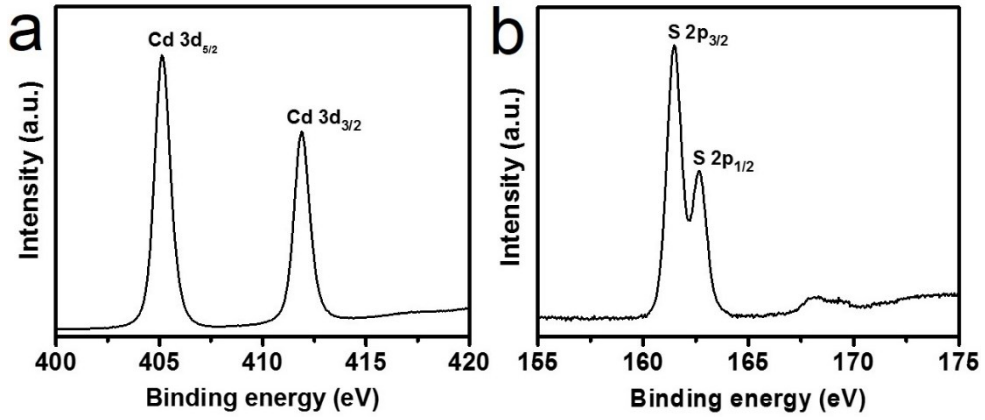

Fig. S3. The characteristic XPS peaks of (a) Cd and (b) S confirm that the as-deposited film on PET substrate is CdS.

4. Raman analysis of CdS films deposited on PET by e-beam evaporation method

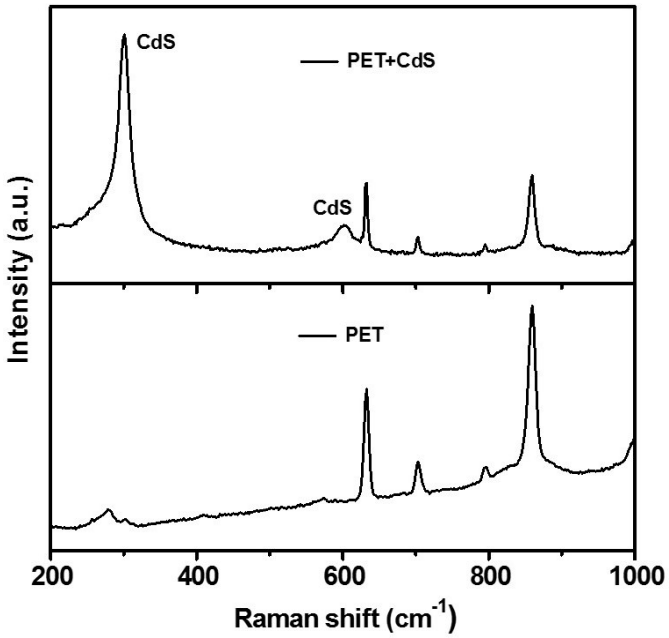

Fig. S4. After subtracting the background of PET substrate, the peaks locating at 302 cm^{-1} and 602 cm^{-1} correspond to the characteristic Raman peaks of CdS, indicating the successful preparation of CdS films.

5. Photograph image of encapsulated CdS films-based photodetectors

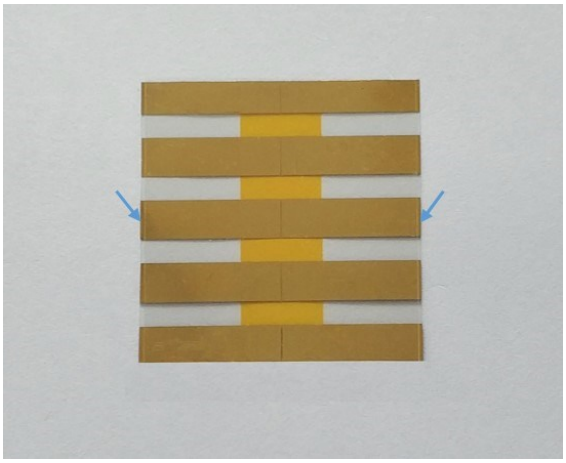

Fig. S5. The photodetector arrays consisting of CdS films (light yellow area) and Au electrodes (dark yellow stripes) on 100-μm-thick PET substrate were encapsulated by another 100-μm-thick PET layer with UV glue. The exposed Au films marked by arrows are used as electrodes. The channel length is about 40 μm.

6. UV–vis absorption of PET and UV glue

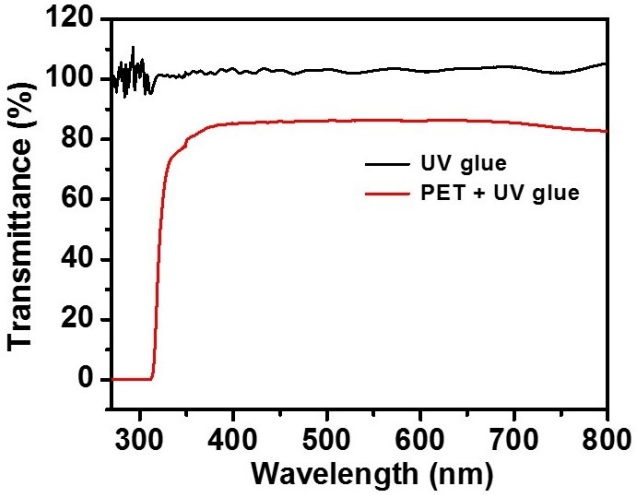

Fig. S6. Based on the UV-vis absorption results, it was found that UV glue are almost transparent for the light from the wavelength of 300 nm to 800 nm, and the used 100-μm-thick PET gives about 20% absorption of the light with wavelength above 325 nm.

7. Photograph image of CdS films-based photodetectors under bending

Fig. S7. Cross-sectional view of the encapsulated CdS films-based device on PET substrate with the size of 3.5 cm × 3.5 cm under bending with the bending radius of approximately 0, indicating that the radius of curvature is about 0.5 cm.

8. Mechanical properties of CdS films-based photodetectors without encapsulation

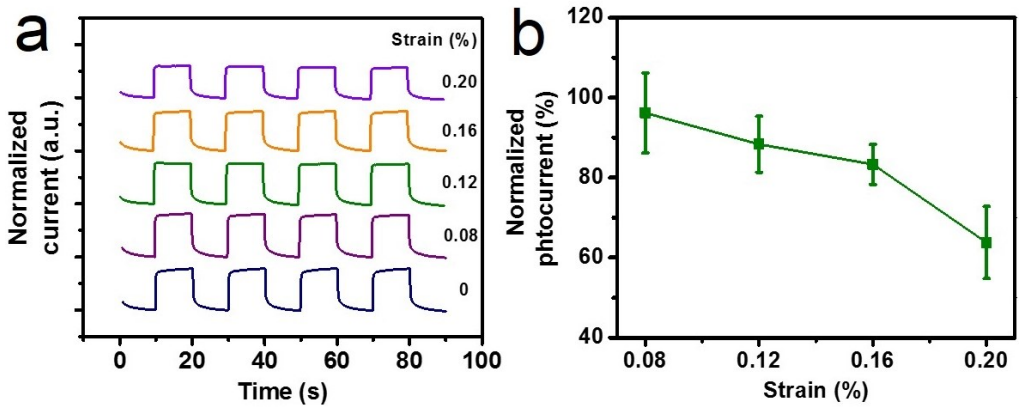

Fig. S8. (a) A time-dependent response of the CdS films-based photodetectors without encapsulation under 365-nm-light illumination with power of 1 mW cm^{-2} at a fixed bias of 1.0 V under bending with different strains from 0 to 0.2%. (b) The corresponding normalized photocurrents of CdS films-based photodetectors varying as the applied strains. It can be seen that CdS films-based photodetectors have a stable performance under the strain of ~0.08%.

9. Time-dependent responses of CdS films-based photodetectors with different t_1/t_2 under bending with radius of curvature of 0.5 cm

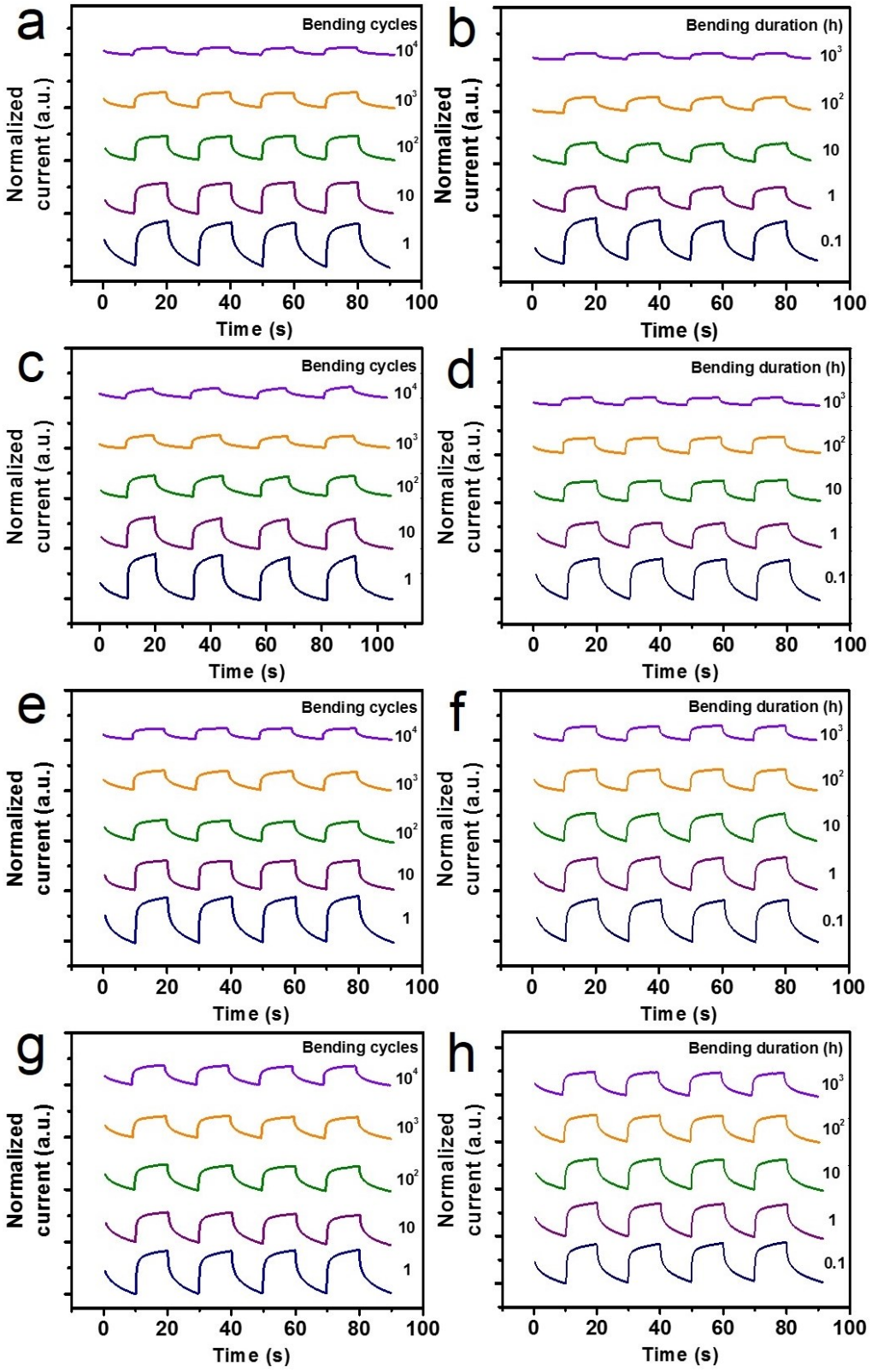

Fig. S9. A time-dependent response of the CdS films-based photodetector on 100-μm-thick PET substrate under 365-nm-light illumination with power of 1 mW cm^{-2} at a

fixed bias of 1.0 V under bending with curvature of 0.5 cm for t_1/t_2=0 with (a) different bending cycles and (b) different bending durations, for t_1/t_2=0.25 with (c) different bending cycles and (d) different bending durations, for t_1/t_2=0.5 with (e) different bending cycles and (f) different bending durations, for t_1/t_2=0.75 with (g) different bending cycles and (h) different bending durations.

10. Optical microscopy and Raman spectroscopy characterization of CdS films after bending

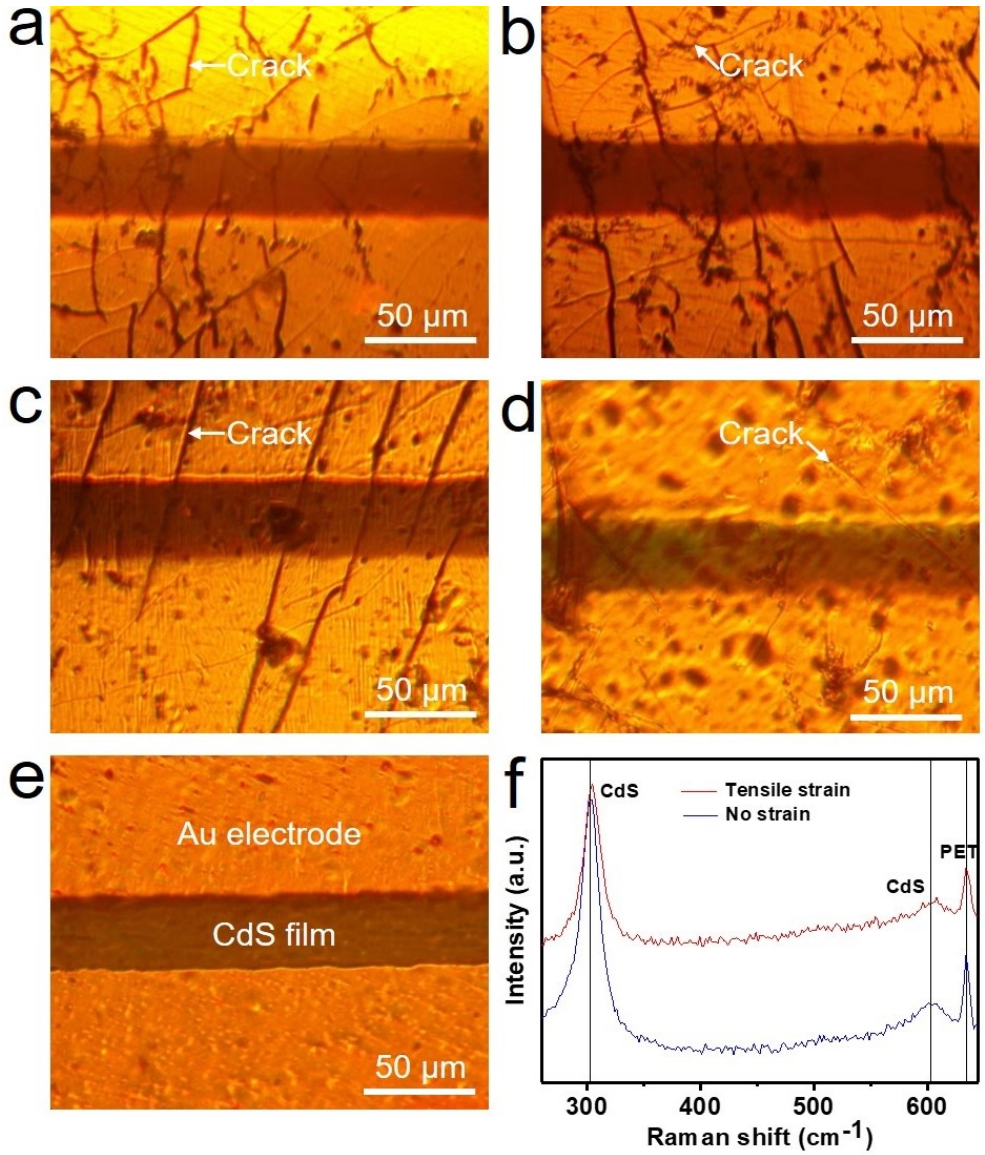

Fig. S10. Optical microscopy images of CdS films on 100-μm-thick PET substrate after bending with curvature of 0.5 cm and with duration of 1000 h for (a) t_1/t_2=0, (b) t_1/t_2=0.25, (c) t_1/t_2=0.5, (d) t_1/t_2=0.75 and (e) t_1/t_2=1. (f) Raman spectra of CdS films

on 100-μm-thick PET substrate without bending and under bending with radius curvature of 0.5 cm. The signal could not be detected in sandwich samples with t_1/t_2=0.25, t_1/t_2=0.5, t_1/t_2=0.75 and t_1/t_2=1 due to the existence of PET layer on top of CdS films.

11. Time-dependent responses of bended CdS films-based photodetectors at neutral mechanical plane with the total thickness of substrate plus encapsulation layer up to 1 mm

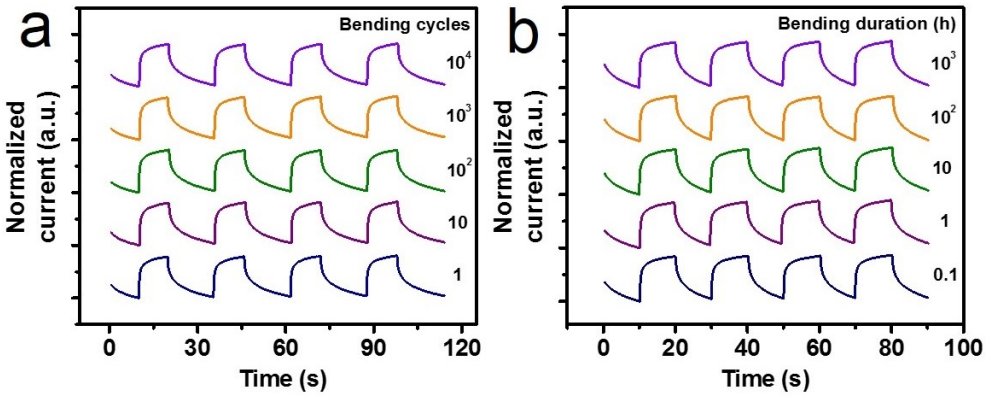

Fig. S11. A time-dependent response of CdS films-based photodetectors under bending with radius of curvature of 0.5 cm after different (a) bending cycles and (b) bending duration on the substrate of 100-μm-thick PET plus 0.5-mm-thick PDMS encapsulated with 100-μm-thick PET plus 0.5-mm-thick PDMS. It can be seen that the devices locating at neutral mechanical plane have ultra-stable performance, in term of the almost unvaried photocurrents.

12. Time-dependent responses of encapsulated photodetectors based on ZnSe, CdSe and NiSe films after bending

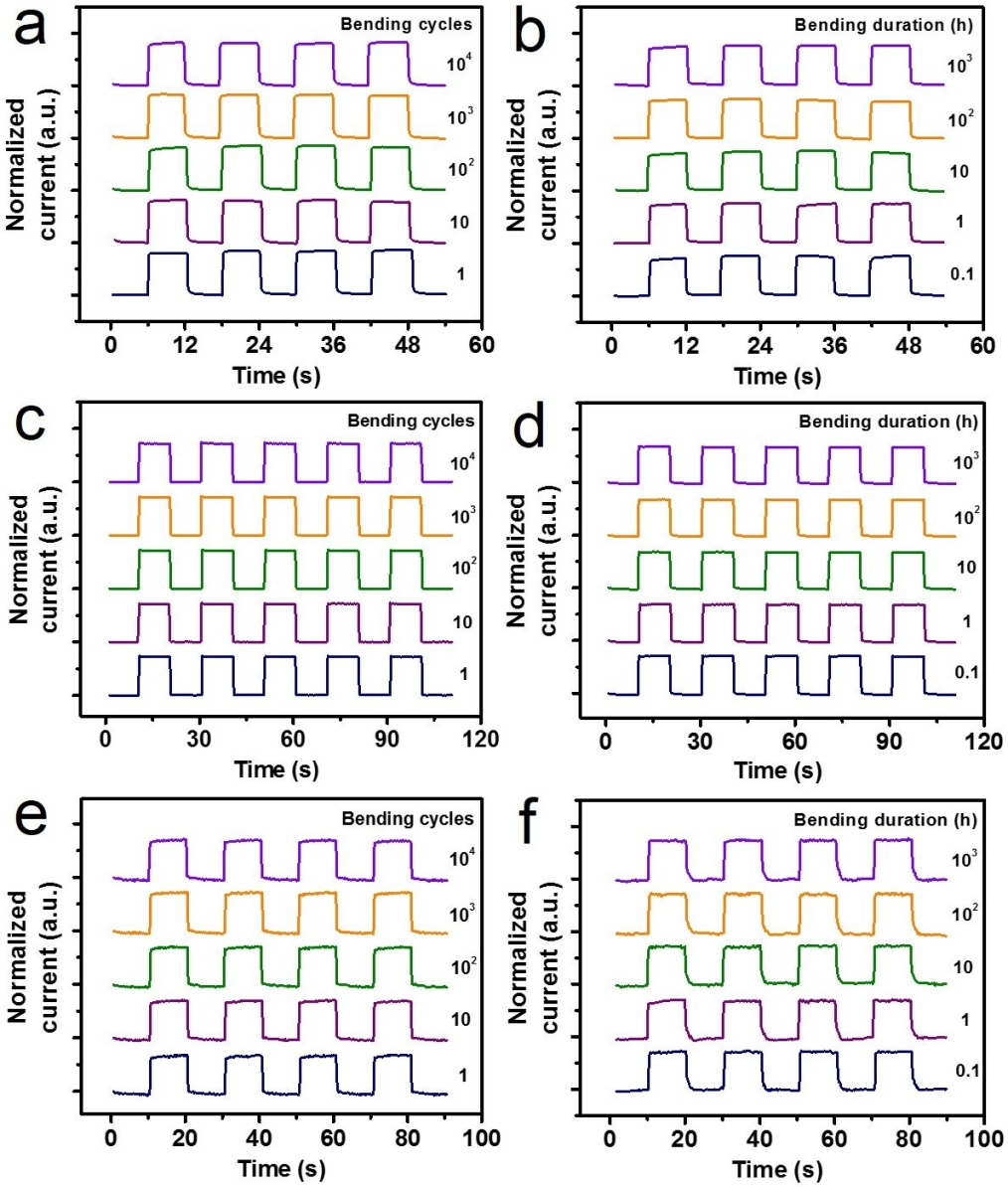

Fig. S12. A time-dependent response of photodetectors at neutral mechanical plane sandwiched by two100-μm-thick PET layer under 365-nm-light illumination with power of 1 mW cm^{-2} at a fixed bias of 1.0 V under bending with radius of curvature of 0.5 cm for CdSe films with (a) different bending cycles and (b) different bending durations, for NiSe films with (c) different bending cycles and (d) different bending durations, for ZnSe films with (e) different bending cycles and (f) different bending durations.

13. Time-dependent responses of photodetectors based on CdS, ZnSe, CdSe and NiSe films after rolling

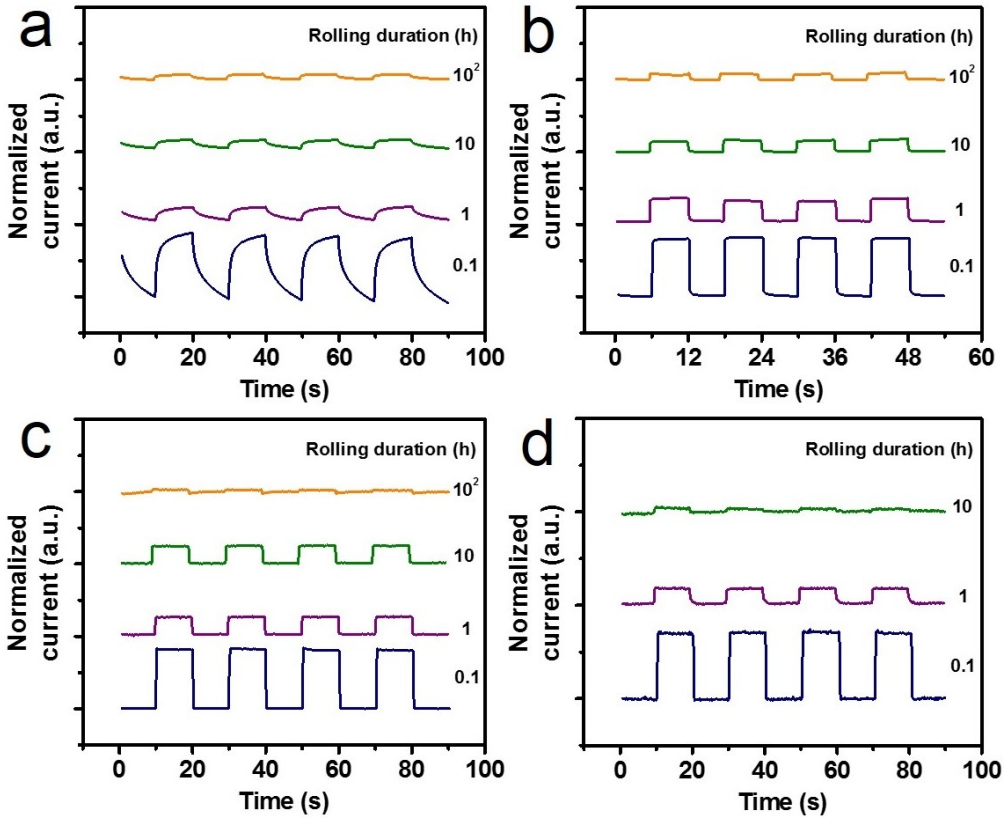

Fig. S13. A time-dependent response of (a) CdS, (b) CdSe, (c) NiSe and (d) ZnSe films-based photodetectors without encapsulation under 365-nm-light illumination with power of 1 mW cm^{-2} at a fixed bias of 1.0 V under rolling with different durations.

14. Time-dependent responses of encapsulated photodetectors based on CdS, ZnSe, CdSe and NiSe films after rolling

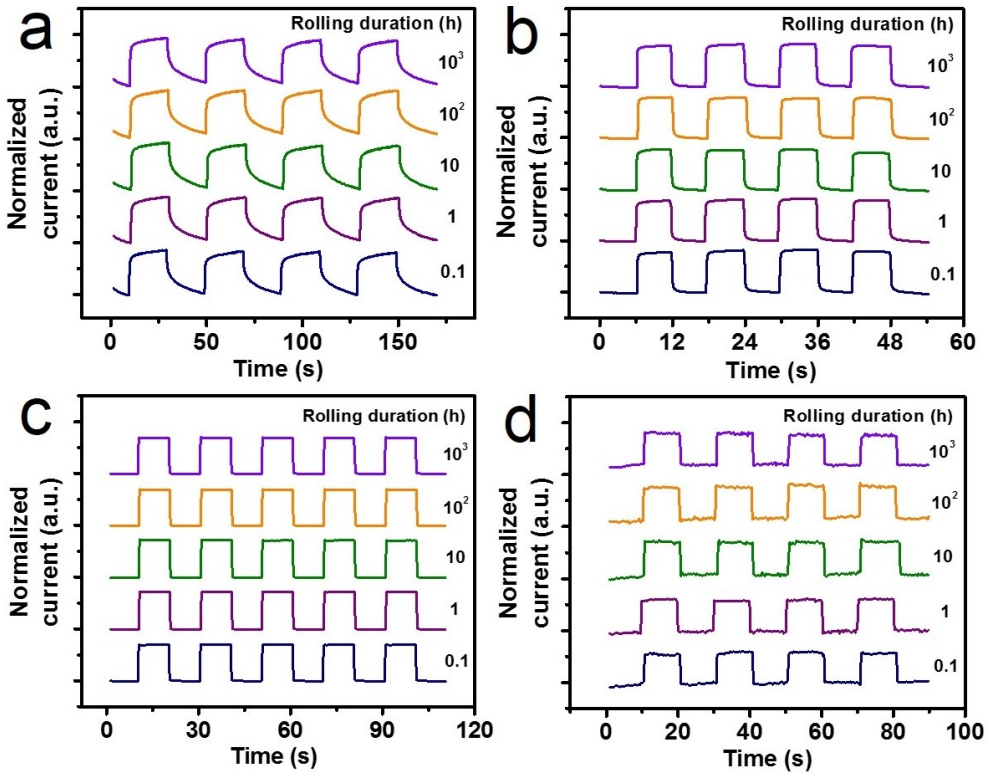

Fig. S14. A time-dependent response of (a) CdS, (b) CdSe, (c) NiSe, and (d) ZnSe films-based photodetectors at neutral mechanical plane sandwiched by two100-μm-thick PET layer under 365-nm-light illumination with power of 1 mW cm^{-2} at a fixed bias of 1.0 V under rolling with different durations.